한국해안 · 해양공학회논문집
제 23 권 제 1 호, pp. 43~49, 2011년 2월

Numerical Analysis of Flow Pattern by Outflow Gates with Manifold Channel
다기수로를 가진 수중 유출구에 의한 유동패턴에 관한 수치해석

Nam Hyeong Kim*, Chang Lym Lee**, Bon Soo Ku*** and Man Soon Song***
김남형* · 이창림** · 구본수*** · 송만순***

Abstract : For the improvement of water quality in a harbor, several studies have been carried out on SEB (Seawater Exchange Breakwater) in recent years, but a problem has been shown whereby the water on the inside area far from the SEB cannot be easily exchanged. In order to solve the problem of the SEB, the Manifold channel, a new concept of the SEB, is introduced in this paper. By using the manifold channel, it is possible to exchange the water of the inside area for seawater from the outside. Here, to assess the outflow gates of the manifold channel governing flow behavior, a virtual manifold channel controlled the location, width and direction of outflow gates applied to the Jumunjin fishery port, where the SEB has been established. In addition, the desirable flow pattern of the port by utilizing the two layer current model is identified, and five general cases of the manifold channel are described in this paper. The model is verified by comparing with observation of the SEB model, and the results are in general agreement. From the results of the manifold channel, in the case of the Jumunjin fishery port, the small circulation of counter clockwise is necessary for the water exchange on the inside area, but it should be controlled by the outflow gates for other areas. Using the two layer current model, the desirable flow pattern of the port can be predicted, and the water exchange for the upper and lower layer can be examined. For the practical use of the manifold channel, further studies on the manifold channel will be necessary, and it may then be used broadly for the design of breakwater in the future.

Keywords : manifold channel, FEM, exchange breakwater, harbor remodeling

요 지 : 최근 친환경항만(Eco-port)을 건설하려는 노력과 쾌적한 워터프론트 개발에 관한 관심이 고조되면서, 항만의 방파제를 중심으로 수질개선을 위한 다양한 연구가 진행되고 있다. 이러한 항 내의 수질개선을 위한 연구로서 최근 해수교환방파제가 주목 받고 있지만, 여전히 항 내 안쪽의 영역에서는 해수교환방파제로부터 유입된 해수가 도달하지 못하여 해수의 순환이 잘 안 되는 단점을 가지고 있다. 본 연구에서는 이러한 해수교환방파제의 단점을 보완하고자, 다기수로라는 새로운 개념의 해수교환방파제를 도입하여, 항 내 안쪽 영역까지 해수의 순환을 촉진할 수 있는 방법을 모색하였다. 이를 위해서 현재 해수교환방파제가 설치된 주문진 항에 가상의 다기수로를 설치하고, 수중유출구의 위치, 크기, 방향을 제어하여 해수유입에 따른 항 내 유동패턴을 비교 검토하고, 해수순환을 촉진시킬 수 있는 방법을 모색하였다.

핵심용어 : 다기수로, 유한요소, 해수교환방파제, 항만 리모델링

1. Introduction

Recently, as the concern for constructing an Eco-port has been increasing internationally, improving water quality at harbors or fishing ports has become an important issue. Several methods have been studied about the issue, and SEB (Seawater Exchange Breakwater) has received attention among these studies in recent years. The SEB is a structure established at the breakwater for exchanging water from the inside area for seawater from the outside. The water quality of the port has then significantly improved where the SEB has been established (Han and Lee, 2006). However, a problem has been revealed whereby the water on the inside area far from the SEB cannot be easily exchanged, so that the water quality in that area remains poor.

In order to solve the problem of the SEB, Manifold channel, a

*제주대학교 토목공학과/해양과환경연구소(Corresponding author: Nam Hyeong Kim, Department of Civil Engineering/Marin & Environmental Research Institute, Jeju National University, Jeju 690-756, Korea, nhkim@jejunu.ac.kr)
**제주대학교 토목공학과(Department of Civil Engineering, Jeju National University, Jeju 690-756, Korea)
***(주) 건화 항만부(Harbor Division, Kunhwa Corporation, Seoul 702-22, Korea)

new concept of the SEB, is introduced in this paper. By using the manifold channel which has several outflow gates on the inside area, it is possible to exchange the contaminated water on the inside area for the seawater from the outside entering through the manifold channel. For the application of the manifold channel on a port, the prediction of the flow behavior due to the inflow current is important, and the manifold channel would be designed more compatibly for the water exchange on the inside area.

In the paper, to assess the outflow gates of the manifold channel governing the flow behavior, a virtual manifold channel is applied to the Jumunjin fishery port, where the SEB has been established, and the desirable flow pattern by utilizing the two layer current model is identified. Controlling the location, width and direction of the outflow gates, a number of cases of the numerical model are carried out, and five general cases are described in the paper, comparing between the flow pattern and the gate conditions. To verify the numerical model, the numerical model of the Jumunjin fishery port with the established SEB is also carried out, and the results are compared with observations.

2. Basic Equation

The coordinates X, Y, Z are illustrated in Fig. 1. In the subsequent development of the two layer current equations, the following notation will be used: U and V are the velocities of the upper and lower layers, η is the water elevation from the mean sea level, b is the depth from the mean sea level to the sea bed, and d is the depth from the mean sea level to the interface level.

The three-dimensional Navier-Stokes equation and Euler's equation of continuity by two layer current are expressed as follows:

$$\dot{U}+U_jU_{i,j}+g\eta_{,i}-v_e(U_{i,j}+U_{j,i})+k_{ij}U_j-\tau_w+\alpha_m(U_i-V_i)=0 \tag{1}$$

$$\dot{\eta}+\dot{d}+\{U_i(\eta+d)\}_{,i}=0 \tag{2}$$

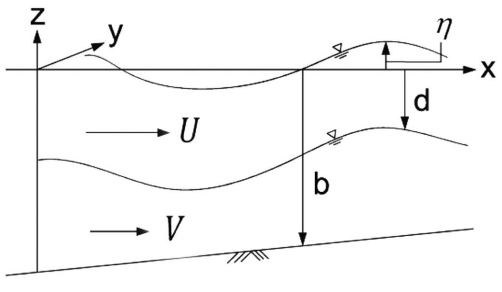

Fig. 1. Two layer model.

$$\left.\begin{aligned}\dot{V}+V_jV_{i,j}+\varepsilon g\eta_{,i}-(1-\varepsilon)gd_{,i}-v_e(V_{i,j}+V_{j,i})_{,j}\\ +k_{ij}V_j+\beta_m(U_i-V_i)+\gamma_mV_i=0\end{aligned}\right\} \tag{3}$$

$$\dot{d}+\{V_i(d-b)\}_{,i}=0 \tag{4}$$

where v_e is the eddy viscosity and ε is the rate of density ($=\rho_u/\rho_l$). Wind stress on the surface τ_w is shown as follows:

$$\tau_w=C_d\rho_\alpha\frac{|W|W_i}{(\eta+d)} \tag{5}$$

where C_d is the drag coefficient (2.55×10^{-3}), ρ_a is the density of air, W is the wind speed 10 m elevation above the sea surface and W_i is the component of the wind speed. k_{ij} is the Coriolis forces shown as follows:

$$k_{ij}=\begin{cases}-f(i=1,\ j=2)\\ f(i=2,\ j=1)\end{cases},\ \text{otherwise zero} \tag{6}$$

where f is the Coriolis parameter. The frictions at the inner boundary and on the bed are expressed as follows:

$$\left.\begin{aligned}\alpha_m&=\frac{f_m}{(\eta+d)\rho_u}\sqrt{(U_1-V_1)^2+(U_2-V_2)^2}\\ \beta_m&=\frac{f_m}{(b-d)\rho_l}\sqrt{(U_1-V_1)^2+(U_2-V_2)^2}\\ \gamma_m&=\frac{f_b}{(b-d)\rho_l}\sqrt{U_1^2-V_1^2}\end{aligned}\right\} \tag{7}$$

where f_m is the kinematic eddy viscosity in the vertical direction, and f_b is the bottom friction coefficient.

3. Finite Element Formulation

Let V be a flow domain. The continuity equations and the momentum equations are employed in the two layer current model in shallow water using the Galerkin method for the discretization of the spatial unknown variables (Kim, 1995; Kim, et al., 2007). For the momentum equations (Eq. (1) and Eq. (3)) and the continuity equations (Eq. (2) and Eq. (4)) that are employed, multiplying both sides of basic equations by the weighting functions, and integrating over the domain V, the finite element solution equations can be derived as follows:

$$\left.\begin{aligned}M_{\alpha\beta}\dot{U}_{\beta i}+K_{\alpha\beta\gamma j}U_{\beta j}U_{\gamma i}+gH_{\alpha\beta i}\eta_\beta+v_e^uR_{\alpha j\beta j}U_{\beta i}+v_e^uS_{\alpha j\beta i}U_{\beta j}\\ +M_{\alpha\beta}k_{ij}U_{\beta j}-T_\alpha\tau_w+M_{\alpha\beta}\alpha_m(U_{\beta i}-V_{\beta i})=0\end{aligned}\right\} \tag{8}$$

$$M_{\alpha\beta}(\dot{\eta}_\beta+\dot{d}_\beta)+B_{\alpha\beta i\gamma}U_{\beta i}(\eta_\gamma+d_\gamma)+C_{\alpha\beta\gamma i}U_{\beta i}(\eta_\gamma+d_\gamma)=0 \tag{9}$$

$$\left.\begin{aligned}M_{\alpha\beta}\dot{V}_{\beta i}+K_{\alpha\beta\gamma j}V_{\beta j}V_{\gamma i}+\varepsilon gH_{\alpha\beta i}\eta_\beta-(1-\varepsilon)gH_{\alpha\beta i}d_\beta+v_e^lR_{\alpha j\beta i}V_{\beta j}\\ +v_e^lS_{\alpha j\beta i}V_{\beta j}+M_{\alpha\beta}k_{ij}U_{\beta j}-M_{\alpha\beta}\beta_m(U_{\beta i}-V_{\beta i})+M_{\alpha\beta}\gamma_mV_{\beta i}=0\end{aligned}\right\} \tag{10}$$

$$M_{\alpha\beta}\dot{d}_{\beta}+B_{\alpha\beta i\gamma}V_{\beta i}(d_{\gamma}-b_{\gamma})+C_{\alpha\beta\gamma i}V_{\beta i}(d_{\gamma}-b_{\gamma})=0 \quad (11)$$

where coefficient matrices are expressed as follows:

$$\left.\begin{aligned} M_{\alpha\beta}&=\int_v(\Phi_\alpha\Phi_\beta)dV,\ K_{\alpha\beta\gamma j}=\int_v(\Phi_\alpha\Phi_\beta\Phi_{\gamma,j})dV\\ H_{\alpha\beta i}&=\int_v(\Phi_\alpha\Phi_{\beta,i})dV,\ R_{\alpha j\beta j}=\int_v(\Phi_{\alpha,j}\Phi_{\beta,j})dV\\ S_{\alpha j\beta j}&=\int_v(\Phi_{\alpha,j}\Phi_{\beta,j})dV,\ B_{\alpha\beta i\gamma}=\int_v(\Phi_\alpha\Phi_{\beta,j}\Phi_\gamma)dV\\ C_{\alpha\beta\gamma i}&=\int_v(\Phi_\alpha\Phi_\beta\Phi_{\gamma,i})dV,\ T_\alpha=\int_v(\Phi_\alpha)dV \end{aligned}\right\}$$

where Φ_α denotes the linear triangular shape function.

For the time discretization, the two-step scheme of Lax-Wendroff is applied (Kawahara, 1976; Kawahara et al., 1982; 1984). From the equations, the unknown variables can be solved simultaneously.

4. Numerical Computation

The 3D bottom bathymetry of the Jumunjin fishery port is shown in Fig. 2. Due to the shallow water depth in the flow domain, the interface elevation of the upper and lower layer is assumed as 3.0 m under the mean sea level at the initial time. With the boundary conditions, it is assumed that the normal velocity to the coastline is zero, and the elevations of incident waves are assumed on the entrance of the port as shown

$$\eta=\sum_{m=1}^{Nc}\left[\alpha_m^u\sin\left\{\frac{2\pi}{T_m}t-k_m\right\}+\alpha_m^l\sin\left\{\frac{2\pi}{T_m}t-k_m\right\}\right]\ \text{on}\ \Gamma_o^u \quad (12)$$

$$d=d_t-\left[\alpha_m^l\sin\left\{\frac{2\pi}{T_m}t-k_m\right\}\right]\ \text{on}\ \Gamma_o^l \quad (13)$$

where N_c is the incident waves number, a_m is the amplitude, k_m is the phase delay, T_m is the period of the M_2, S_2, K_1 and Q_1 constituents, t is the time increment in computation and d_t is the depth from the mean sea level to the interface level at t, respectively. The harmonic analysis of M_2, S_2, K_1 and Q_1 in the Jumunjin fishery port is shown in Table 1. Also, in the case of the Jumunjin fishery port, for the strong current of incident waves, the observed velocity (DRMAFO, 2004; 2005) is assumed at the entrance of the port, and the flux of the inflow and outflow on the port is controlled.

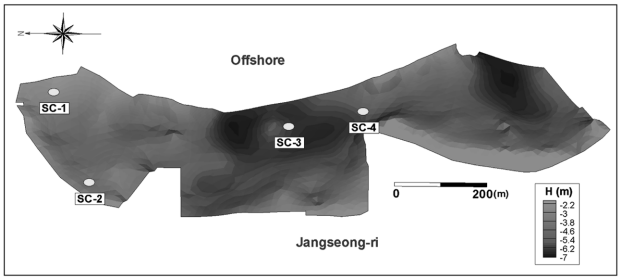

Fig. 2. 3D bottom bathymetry of Jumunjin fishery port with observation nodal point.

Table 1. Results of the harmonic analysis for tide in Jumunjin fishery port (MOMAF, 1999)

N_c	Constituent	Amplitude α_m (cm)	Period T_m (hour)	Phase delay k_m (degree)
1	M_2	6.94	12.4206	91.486
2	S_2	1.79	12.0000	120.689
3	K_2	4.35	23.9344	1.367
4	O_1	4.70	25.8193	320.935

4.1 Verification of the Numerical Model

To verify the numerical model, a two layer current model of the Jumunjin fishery port with SEB is carried out. From the SEB, the inflow condition of seawater is given as 0.5 m/s, which was observed by DRMAFO (2005) in the conduction pipe. As the SEB uses the waves overflowing the wall of an arch, it is assumed that the water of the upper layer is exchanged for the seawater while the sea level is higher than mean sea level, and the flux of the inflow is set to be the maximum value at the high tide. The velocity vectors of the SEB at the high tide are shown in Fig. 3. For the weak tidal current, the inflow from the SEB flows toward the entrance of the port. Except for the partial area, this figure shows good water exchanging at the Jumunjin fishery port.

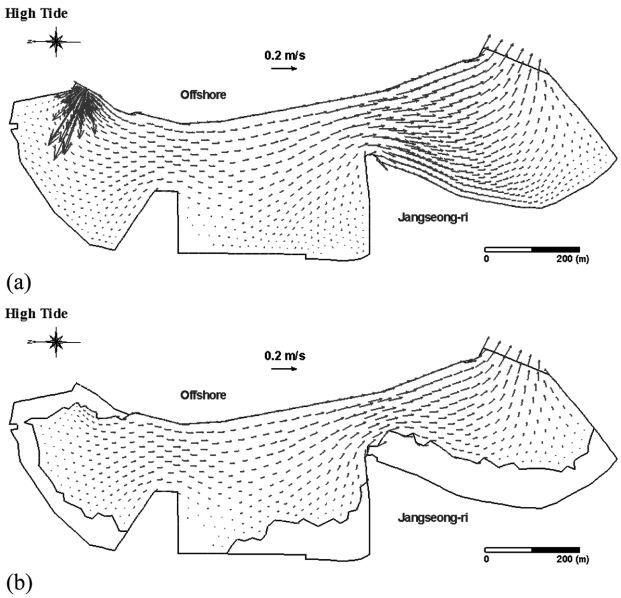

Fig. 3. Velocity vectors of Jumunjin fishery port with SEB: (a) upper layer (b) and lower layer.

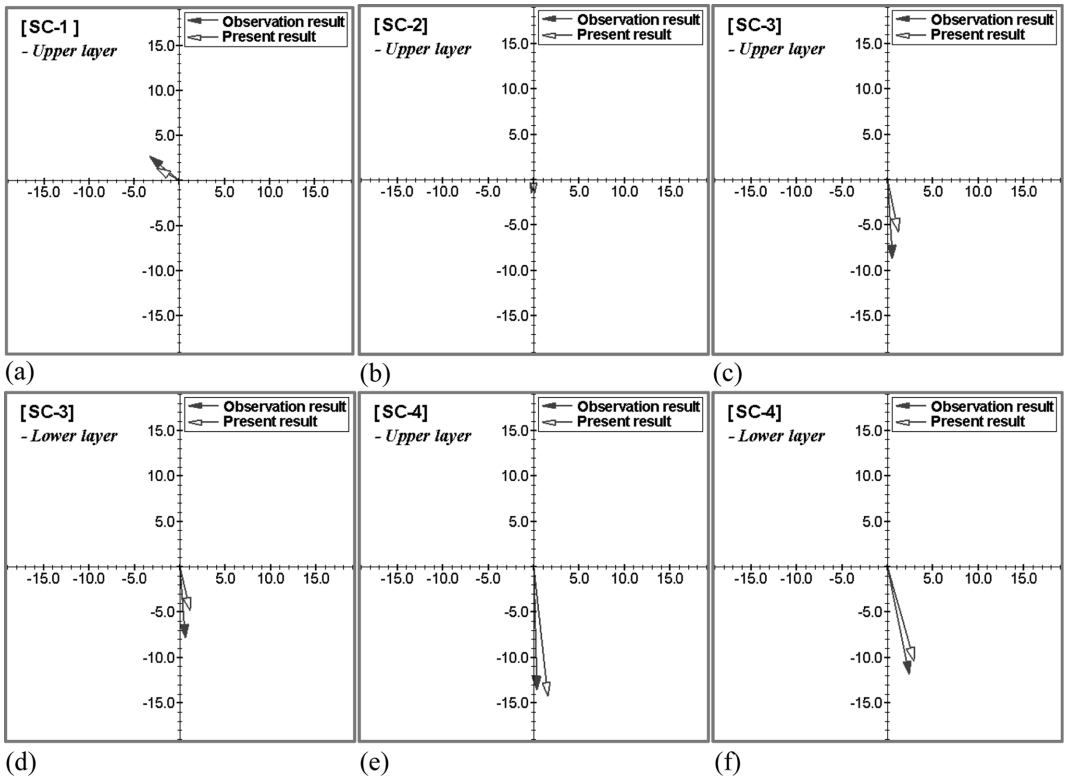

Fig. 4. Comparison of velocity vectors with computed results and observation results at nodal points of (a) SC-1; (b) SC-2; (c), (d) SC-3; (e), (f) SC-4.

The computed results are compared with the observations, which were observed by Sea Tech R&D (2008) at the nodal points shown in Fig. 2, and the comparisons are shown in Fig. 4. For the case where the depth of the seabed at the nodal points of SC-1 and SC-2 is shallower than the interface level, these velocities of the lower layer cannot be calculated in this model. From the comparisons, it is seen that these results agree well with the observations. At the nodal point of SC-3, the computed velocity is weaker than the observation, however the tendency of velocity is the similar to the observation. Therefore, this model can be applied for the simulation of the Jumunjin fishery port.

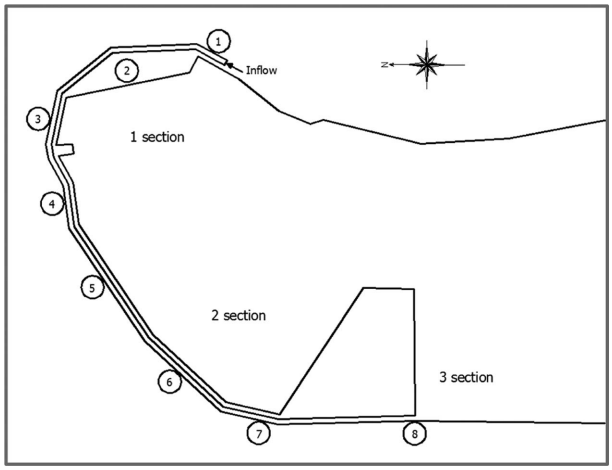

Fig. 5. Gate position of manifold channel.

4.2 Examination of Flow Pattern by Manifold channel

For examination of the flow pattern of the port, a virtual manifold channel is established in the Jumunjin fishery port. Fig. 5 and Fig. 6 demonstrate the outflow gates of the manifold channel. As shown in Fig. 5, the dimensions of the manifold channel are assumed length of 762.1 m, width of 5.3 m and depth of 2.0 m, and the outflow gates are located at the general eighth position on the inside area of the port. In this paper, the position and number of the gates are controlled, and the outflow gates, which can exchange the water in Section 1 to 3, are determined. Also, the direction and width of the gate are controlled: the direction is set between 0 and 180 degrees based on the flow direction, and the width is assumed to be a certain distance, as shown in Fig. 5.

In a relatively small area such as the manifold channel, if the area consists of a single element, the application of the slip boundary condition might cause a slight difference in the numerical analysis, because all of the nodes are under the boundary condition. Therefore, by utilizing the automatic mesh generation method developed by Kim et al. (2010), the differential partition of the finite mesh is applied, and

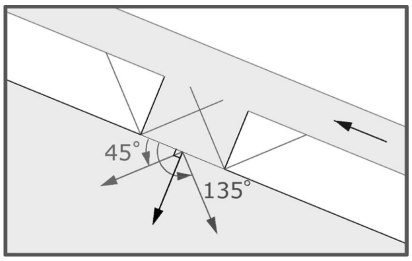

(a)

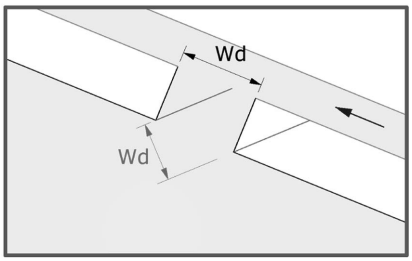

(b)

Fig. 6. Definition sketch of outflow gate of (a) direction (b) and width.

the manifold channel can consist of more than two elements, as shown in Fig. 7.

A number of manifold channel models are carried out, controlling outflow gate conditions; one of the velocity vector by using manifold channel, which has gate numbers 3, 4, 6 and 8, is presented in Fig. 8. As shown in this figure, it is seen that the inflow from the SEB flows toward the entrance of the port, and the basin near the entrance is flushed. Also, the flow pattern of the lower layer shows that the water of the lower layer can be exchanged due to the inflow of the upper layer. Since most cases of the manifold channel are much alike in flow pattern near the entrance and in the lower layer, the general five cases of velocity vectors of the upper layer focused on inside area are shown in Fig. 9(a) to (e). In comparison with the gate position of the manifold channel, gate numbers 3, 4, 6 and 8 lead to the appropriate flow pattern for the water exchange of inside area as shown in Fig. 8 and Fig. 9(a). Suppose the total number of gates is small, the velocity near Section 3 is increased but the velocities of Sections 1 and 2 are decreased. Therefore, three or four gates are approximately required on the inside area. Also, with a small number of gates, it is possible to increase the velocity of the outflow from the gates, but this may lead to an inappropriate flow pattern for the water exchange on the inside area, so that the suitable gate number would be necessary.

Fig. 9(b) and Fig. 9(c) show the velocity vectors controlling the direction of the gates. From the computed results for controlling the position and number of gates, it can be seen that Section 1 shows good water exchange, but the water of Section 2 cannot be easily exchanged due to the weak velocity of the outflow. In the case of Section 2, though the outflow gates are located in the area, the water of the

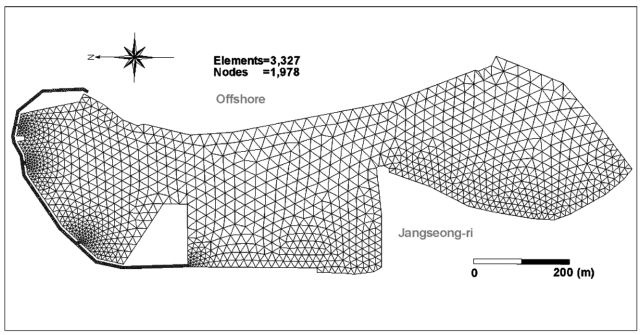

(a)

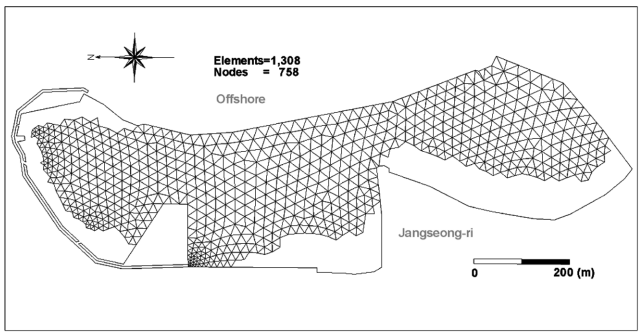

(b)

Fig. 7. Finite element idealization of Jumunjin fishery port with manifold channel: (a) upper (b) and lower layer.

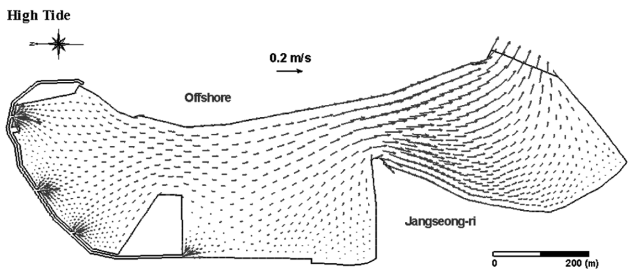

(a)

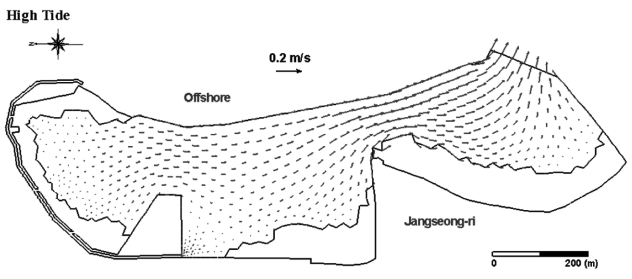

(b)

Fig. 8. Velocity vectors of Jumunjin fishery port with manifold channel: (a) upper (b) and lower layer.

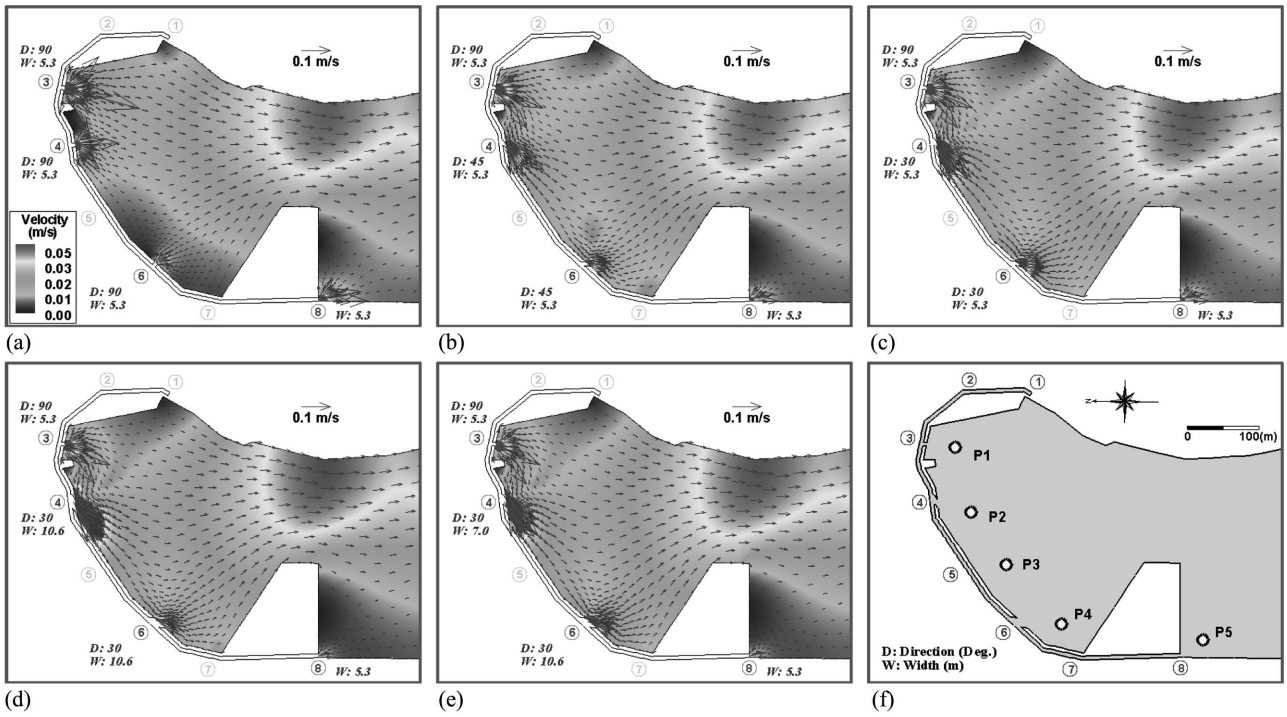

Fig. 9. Velocity vectors focused on inside area with gate number 3, 4, 5 and 8 (a) Case 1: width 5.3 m, direction 90° (b) Case 2: controlled direction of gate 4 and 8 as 45° (c) Case 3: controlled direction of gate 4 and 8 as 30° (d) Case 4: controlled width of gate 4 and 8 as 10.6 m (e) Case 5: controlled width of gate 4 as 7.0 m; (f) nodal points for comparison of computed result.

outflow from the gates flows to the entrance of the port directly, and only the partial area where the outflow gate is established is exchanged, indicating that more outflow gates are necessary in this area and these existing gates are not effective. Therefore, controlling the direction of the existing gates, the circulation of counter clockwise is weakly formed, causing an increase in the velocities of the area near Section 2. However, the decrease of the velocity on Section 1 can be caused by the circulation, it would be controlled.

Fig. 9(d) and Fig. 9(e) show the velocity vectors controlling the width of the gates. In order to control the appropriate flow pattern of the port and maintain the velocity from the outflow gate on Section 3, the width of the gates is controlled, and the outflow flux from the gates can be distributed evenly.

For the examination of the gate conditions, the velocities of the nodal points in Fig. 9(f) are compared, and the comparison is shown in Fig. 10. It is seen that the velocities of Case 5 are increased more evenly and the gate conditions of manifold channel, Case 5, are suitable in the Jumunjin fishery port for the water exchange.

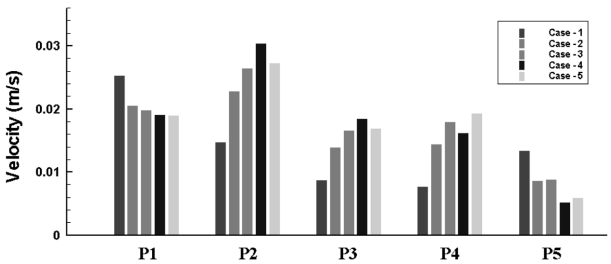

Fig. 10. Comparison of velocity of computed results at nodal points.

5. Conclusions

In this study, a numerical model of the Jumunjin fishery port by a two layer current is carried out, and the flow patterns of the port due to the outflow gates are identified, controlling the location, direction and width of the gates. The main results of the present study are listed below:

(1) To verify the two layer current model, the computed results of the SEB are compared with observations, and this shows that the results of the model are in general agreement with the observations. Thus, the numerical analysis by the two layer current model is verified.

(2) For the comparisons of the flow pattern, due to the characteristic of the Jumunjin fishery port, the relation can be obtained as follows: as the circulation of counter clockwise is formed on the inside area, the velocity of Section 2 is increased, while the velocity of Section 1 is decreased; that is, the velocities of Section 1 and 2 are conflicting with the circulation. Thus, the circulation should be controlled appropriately, and the velocities of both sections should be increased.

(3) From the examination of the flow patterns, by using the two layer current model, the desirable flow pattern of the Jumunjin fishery port, as shown in Fig. 9(e), is yielded.

For the practical use of the manifold channel, further studies on the manifold channel would be necessary; the manifold channel might then be able to be used broadly for the design of breakwater in the future.

Acknowledgement

This work is based on the projects for “Establishment of the foundation for harbor remodeling”, supported by the Ministry of Land, Transport and Maritime Affairs (MLTM).

References

Donghae Regional Maritime Affairs & Fisheries Office (2004). Final report of preparatory monitoring investigation of Jumunjin fishery port, Korea Ocean Research & Development Institute, Korea (in Korean).

Donghae Regional Maritime Affairs & Fisheries Office (2005). Final report of monitoring investigation of Jumunjin fishery port 2nd, Korea Ocean Research & Development Institute, Korea (in Korean).

Han, D.J. and Lee, D.S. (2006). Effect of water quality improvement by seawater exchange breakwater install. Korean J. Sanitation, Vol. 21, No. 3. 61-72 (in Korean).

Kawahara, M. (1976). Convergence of finite element Lax-Wendroff method for linear hyperbolic differential equation. Proc. of JSCE, No. 253, 95-107.

Kasahara, K., Hara, H. and Kawahara, M. (1984). Two-step explicit finite element method for two-layer flow analysis. Int. J. Numer. Meth. Fluids, Vol. 4, 931-947.

Kawahara, M., Hirano, H., Tsubota, K., and Inagaki, K. (1982). Selective lumping finite element method for shallow water flow. Int. J. Numer. Meth. Fluids, Vol. 2, 89-112.

Kim, N.H. (1995). An analysis of shallow water flow by two step explicit finite element scheme. J. of the Korean Society of Civil Eng., Vol.15, No.6, 1669-1677.

Kim, N.H., Park, J.H., and Kang, H.W. (2007). The numerical analysis of Jeju harbor flow considering effect of seasonal wind. J. of Korean Navigation and Port Research, Vol. 31, No. 9, 793-799 (in Korean).

Kim, N.H., Yun, H.C. and Hur, Y.T. (2010). Development of generating technique for triangular mesh by using distinct element method. J. of Korean Navigation and Port Research, Vol. 34, No. 5, 367-373 (in Korean).

Ministry of Maritime Affairs and Fisheries (1999). Research for exchange breakwater to practical use (II). Korea Ocean Research & Development Institute, Korea (in Korean).

Sea Tech R&D (2008). Report of ocean survey for exchange breakwater on Jumunjin fishery port. (in Korean).

원고접수일: 2010년 8월 25일
수정본채택: 2010년 11월 19일
게재확정일: 2010년 12월 13일